Nonreciprocal Metamaterial Obeying Time-Reversal Symmetry

Siddharth Buddhiraju⬤, Alex Song, Georgia T. Papadakis, and Shanhui Fan
*Ginzton Laboratory, Department of Electrical Engineering, Stanford University,
Stanford, California 94305, USA*

We introduce a class of non-Hermitian systems that break electromagnetic reciprocity while preserving time-reversal symmetry, and describe its novel polarization dynamics. We show that this class of systems can be realized using van der Waals heterostructures involving transition-metal dichalcogenides (TMDs). Our work provides a path towards achieving strong optical nonreciprocity and polarization-dependent directional amplification using compact, large-area and magnet-free structures.

Introduction.—Metamaterials enable us to create systems with effective permittivity and permeability that are not found in nature [1–9], opening up new possibilities for manipulating the properties of electromagnetic waves. In general, the allowed forms of the permittivity and permeability tensors are strongly constrained by symmetry considerations. For a nonmagnetic medium with $\mu = 1$, the constraints of energy conservation, time-reversal symmetry ($\mathcal{T}$), and reciprocity (R) are represented by $\epsilon^\dagger = \epsilon$, $\epsilon^* = \epsilon$, and $\epsilon^T = \epsilon$, respectively. Here the exponents $\dagger$, $*$, and T denote the Hermitian conjugate, complex conjugate, and transpose, respectively. These constraints are related in that any two imply the third. Consequently, in linear, time-invariant media, exactly five classes of dielectric tensors are possible: (1) usual, lossless dielectrics, which satisfy all three conditions, (2) usual, lossy dielectrics, which satisfy only $\epsilon^T = \epsilon$ but not the other two, (3) lossless nonreciprocal media such as idealized magneto-optical materials, which satisfy only $\epsilon^\dagger = \epsilon$, (4) nonreciprocal media with time-reversal symmetry, which satisfy only $\epsilon^* = \epsilon$, and (5) media that violate all three constraints. Somewhat surprisingly, among these five classes of materials, there have not been in fact any previous studies of materials or metamaterial systems that belong to class (4), while all other classes of dielectric tensors have been extensively explored.

In this Letter, we explore nonreciprocal metamaterial systems that possess time-reversal symmetry. Such systems are, by necessity, non-Hermitian. We first derive the polarization dynamics of such media from their eigenvalues and eigenstates. It will be seen that they possess two distinct phases separated by an exceptional point, akin to $\mathcal{PT}$-symmetric systems. These phases exhibit direction- and polarization-dependent gain and loss and arbitrary polarization conversion for pairs of polarization states, respectively. We show that in the "broken" phase, such media could be used to construct a unique two-way directional amplifier whose direction of amplification depends on the incident polarization. Then, we design a

van der Waals heterostructure using transition-metal dichalcogenide (TMD) layers that realizes the proposed dielectric tensor. We conclude with a brief discussion of such nonmagnetic schemes to achieve nonreciprocal behavior.

We first outline an important consequence of time-reversal symmetry in such media. Suppose that light of a given polarization propagating through such a medium is amplified by a factor g in one direction. Since the medium obeys $\mathcal{T}$ symmetry, the complex-conjugated polarization must be attenuated by the same factor g when propagating in the reverse direction. For example, this means that a given linear polarization amplified in forward propagation is attenuated by the same factor in reverse propagation, making the system nonreciprocal. This property distinguishes this class of systems from other non-Hermitian media such as $\mathcal{PT}$-symmetric systems and nonreciprocal directional amplifiers that do not obey $\mathcal{T}$ symmetry.

To analyze the properties of such media, we begin with a dielectric tensor of the form

$$\bar{\epsilon} = \begin{pmatrix} \epsilon_{xx} & \epsilon_{xy} & 0 \\ \epsilon_{yx} & \epsilon_{yy} & 0 \\ 0 & 0 & \epsilon_{zz} \end{pmatrix}. \tag{1}$$

Under normal incidence, i.e., for propagation along the $\hat{z}$ direction, the relevant part of $\bar{\epsilon}$ is

$$\epsilon_\perp = \begin{pmatrix} \epsilon_{xx} & \epsilon_{xy} \\ \epsilon_{yx} & \epsilon_{yy} \end{pmatrix}. \tag{2}$$

The full set of constraints on the elements of $\epsilon_\perp$ under time-reversal symmetry, reciprocity and Hermiticity are outlined in the Supplemental Material [10] (Secs. I–II). Here, since the medium of interest is $\mathcal{T}$ symmetric and nonreciprocal, we require all elements of $\epsilon_\perp$ to be real to preserve $\mathcal{T}$ symmetry and $\epsilon_{xy} \neq \epsilon_{yx}$ to break reciprocity. For simplicity, we assume $\epsilon_{xx} = \epsilon_{yy} \equiv \epsilon_r$. Assuming a field solution of the

form $\mathbf{E}_0 e^{-ik_z z}$, Maxwell's equations in this medium result in the eigenvalue problem

$$k_z^2 \mathbf{E}_0 = \frac{\omega^2}{c^2} \epsilon_\perp \mathbf{E}_0. \tag{3}$$

The polarization dynamics, i.e., the evolution of the polarization of light as it propagates through this medium, is governed by the eigenvalues and eigenstates of $\epsilon_\perp$. With $\tau = \epsilon_{yx}/\epsilon_{xy}$, the eigenvalues of $\epsilon_\perp$ are

$$\epsilon_\pm = \epsilon_r \pm \epsilon_{xy}\sqrt{\tau}, \tag{4}$$

and the right eigenstates are

$$|v_\pm^R\rangle = \frac{1}{\sqrt{2}}\begin{pmatrix} 1 \\ \pm\sqrt{\tau} \end{pmatrix}. \tag{5}$$

At normal incidence, the two polarizations $|v_\pm^R\rangle$ propagate with wave vectors $k_{z\pm} = k_0\sqrt{\epsilon_\pm}$, where $k_0 = \omega/c$ is the propagation constant in vacuum. The ratio τ serves as an indicator of broken reciprocity in the medium, since $\epsilon_{yx} \neq \epsilon_{xy}$ corresponds to a nonreciprocal system. The normalization of $|v_\pm^R\rangle$ is set using $\langle v_\pm^L|v_\pm^R\rangle = 1$, where the left eigenstates $\langle v_\pm^L|$ are defined by the eigenvalue problem $\langle v_\pm^L|\epsilon_\perp = \epsilon_\pm \langle v_\pm^L|$.

From Eq. (4), it is seen that this class of materials possess, in analogy to $\mathcal{PT}$-symmetric systems [12,13], an exact and a broken phase separated by an exceptional point. The exceptional point occurs at $\tau = 0$, where the eigenstates coalesce into a single linear polarization. In the broken phase of $\tau < 0$, the eigenstates are two elliptical polarizations experiencing equal gain and loss, respectively. The polarization dynamics in this regime are depicted on the Poincaré sphere in Fig. 1(a) for $\tau = -1$. Since the polarization state $|v_+^R\rangle$ experiences gain while $|v_-^R\rangle$ experiences loss, all initial polarization states except $|v_-^R\rangle$ amplify and rotate towards $|v_+^R\rangle$ as they propagate through the medium, depicted by the yellow trajectories on the sphere. By contrast, in the exact phase of $\tau > 0$, the eigenvalues in Eq. (4) are real, corresponding to two linear but nonorthogonal polarizations. In this phase, when any polarization state other than $|v_\pm^R\rangle$ is injected into the medium, its polarization precesses about the eigenstates $|v_\pm^R\rangle$ as it propagates, as shown in Fig. 1(b). Moreover, the medium continues to have gain even though neither of $\epsilon_\pm$ has an imaginary part. This can be verified from the Poynting flux, which oscillates with propagation distance but can exceed the power in the initial state (see Supplemental Material [10], Sec. III). Furthermore, since the polarization of light precesses around nonorthogonal states, such a medium can transform arbitrary pairs of input polarization states into orthogonal states when the thickness of the medium is chosen appropriately, enabling the construction of highly sensitive polarization-detectors. This
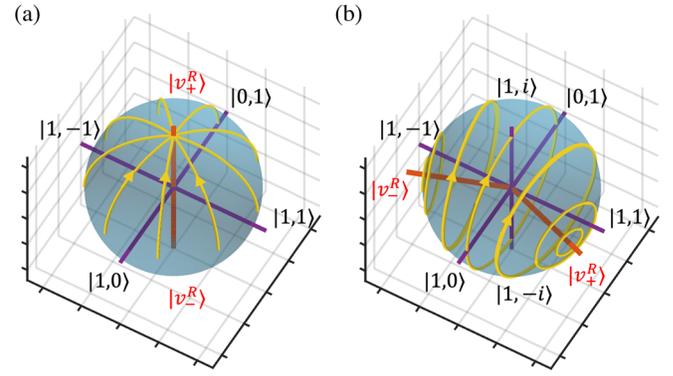

FIG. 1. Poincaré spheres describing the polarization dynamics as light travels through the medium of Eq. (2) when (a) $\tau = -1$, and (b) $\tau = +2$, where $\tau = \epsilon_{yx}/\epsilon_{xy}$. When $\tau < 0$, all initial polarizations except $|v_-^R\rangle$ amplify to $|v_+^R\rangle$ as they propagate through the medium. For $\tau > 0$, the polarization precesses in circles around the nonorthogonal states $|v_\pm^R\rangle$.

property was first noted in Ref. [12] for $\mathcal{PT}$-symmetric systems, but extends readily to the media in this Letter since it depends only on the nonorthogonality of the eigenstates.

When considering propagation in only one direction, the media discussed in this Letter may appear analogous to other non-Hermitian media such as $\mathcal{PT}$-symmetric systems [12]. However, in sharp contrast to the $\mathcal{PT}$-symmetric systems of Ref. [12], which inherently break time-reversal symmetry while preserving reciprocity, the media under consideration in this Letter preserve time-reversal symmetry and break reciprocity, resulting in unique properties. Notice that in the permittivity tensor of Eq. (2), for $\tau < 0$, if light of a certain polarization is amplified in forward propagation, its complex conjugate polarization is attenuated by the same factor in reverse propagation, unlike $\mathcal{PT}$-symmetric systems. This is clearly seen from Eqs. (4) and (5), since $k_{z+}^* = k_{z-}$ and $|v_+^R\rangle^* = |v_-^R\rangle$ for $\tau < 0$. By contrast, when $\tau > 0$, the material provides nonreciprocal rotation of polarization. For instance, when the thickness of the medium is chosen to be $d = \pi/2(k_{z+} - k_{z-})$, an initial polarization state $|x\rangle$ inserted on one end of the medium is rotated and amplified to $\sqrt{\tau}|y\rangle$ on the other end. On the other hand, a $|y\rangle$-polarized initial state inserted back from the other end is rotated and attenuated to $\sqrt{\tau}^{-1}|x\rangle$, making the medium nonreciprocal. Notice that because the factors $\sqrt{\tau}$ and $\sqrt{\tau}^{-1}$ cancel each other, the medium continues to preserve $\mathcal{T}$ symmetry.

The presence of time-reversal symmetry in a non-Hermitian system can have interesting consequences. For example, we show that such media can realize a unique polarization-dependent two-way directional amplifier. In previous works on directional amplification [14–20], light propagating in one direction is amplified while that in the reverse direction is attenuated. By contrast, the media considered in this work can realize directional amplification for two orthogonal polarizations in opposite directions.
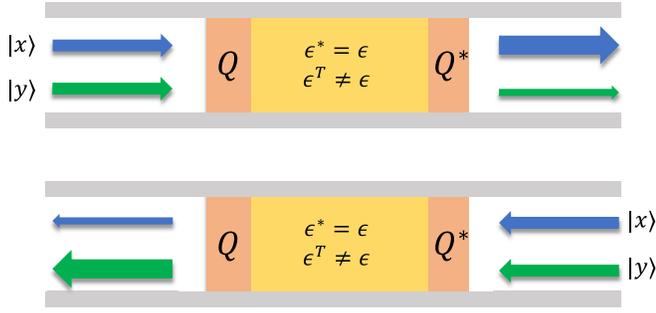
FIG. 2. Schematic of a communication channel with the $\mathcal{T}$-symmetric metamaterial (yellow) sandwiched between two linear-to-circular polarization converters (orange) with orthogonal fast axes. In forward propagation (top panel), an $|x\rangle$-polarized signal is converted to $|v_+^R\rangle$, amplified, and rotated back to $|x\rangle$, whereas a $|y\rangle$-polarized signal is rotated to $|v_-^R\rangle$, attenuated, and rotated to $|y\rangle$. In reverse propagation (bottom panel), owing to $\mathcal{T}$ symmetry of the structure, an $|x\rangle$-polarized signal is attenuated while a $|y\rangle$-polarized signal is amplified.

This property can be used in a two-way communication channel, where communication in the forward direction $(+\hat{z})$ is in, say $|x\rangle$ polarization, while that in the backward direction $(-\hat{z})$ is in $|y\rangle$ polarization. Suppose we intend to build a repeater for such a channel, so that $|x\rangle$-polarized light is amplified along $+\hat{z}$ while $|y\rangle$-polarized light is amplified along $-\hat{z}$. Simultaneously, we would like any reflections or noise in $|x\rangle$ polarization to be attenuated in the $-\hat{z}$ direction, and in $|y\rangle$ polarization in the $+\hat{z}$ direction. The schematic for a single unit of such a repeater is shown in Fig. 2. This configuration can be achieved using the medium described by Eq. (2) with $\epsilon_{xy} = -\epsilon_{yx}$, shown by the purple layer, sandwiched between two linear-to-circular polarization converters (e.g., quarter-wave plates) depicted the by orange layers. Since $\tau = \epsilon_{yx}/\epsilon_{xy} = -1$, the eigenstates of the medium from Eq. (5) are the two circular polarizations $|v_\pm^R\rangle$, experiencing equal amplification and attenuation, respectively. The two linear-to-circular converters have orthogonal fast-axes and are described using transmission matrices Q and Q^*, respectively, where

$$Q = \frac{1}{\sqrt{2}} \begin{pmatrix} 1 & i \\ i & 1 \end{pmatrix}. \tag{6}$$

Suppose an $|x\rangle$-polarized signal is inserted into the channel along the $+\hat{z}$ direction. The converter Q rotates $|x\rangle$ to $Q|x\rangle = |v_+^R\rangle$, which is then amplified by the medium. The amplified $|v_+^R\rangle$ signal is then rotated back to an amplified $|x\rangle$ signal by the converter Q^*. Since the entire system preserves $\mathcal{T}$ symmetry, any noise or reflection in the $|x\rangle$ polarization traveling along the $-\hat{z}$ direction is attenuated by the medium. Furthermore, since the two polarization converters Q and Q^* have staggered fast axes, a $|y\rangle$ signal traveling along the $-\hat{z}$ direction is converted to $Q^*|y\rangle = -i|v_+^R\rangle$, amplified by the

same factor, and rotated back to an amplified $|y\rangle$ signal by the converter Q. Again, by $\mathcal{T}$ symmetry, any noise in the $|y\rangle$ polarization traveling along the $+\hat{z}$ direction is attenuated (see the Supplemental Material [10], Sec. IV for a detailed analysis). Therefore, this setup realizes a novel two-way directional-amplifier, whose direction of amplification depends on the injected polarization, and can be used to achieve enhanced signal-to-noise ratio of two-way signal transmission using orthogonal polarizations.

As another application, photonic lattices with an imaginary gauge potential [21] have been shown to demonstrate effective unidirectional light transport originating from non-Hermitian delocalization [22,23]. Since the $\mathcal{T}$-symmetric media considered here possess direction-dependent amplification and attenuation, they provide a pathway to physically implement an imaginary gauge potential.

Metamaterial design.—Having discussed the polarization dynamics and potential applications of such media, we propose a metamaterial design that realizes the general form of Eq. (2). We start with the special case of Eq. (2) with $\epsilon_{xy} = -\epsilon_{yx}$. Here, it is seen from Eqs. (4) and (5) that the medium exhibits circular-polarization-dependent gain and loss. To generate this behavior, van der Waals heterostructures consisting of transition-metal dichalcogenides (TMD) monolayers are ideal candidates owing to their unique valley-dependent optical properties. TMD monolayers are gapped Dirac materials with a direct bandgap in the visible [24]. The broken inversion-symmetry in these monolayers results in the locking of spin and valley degrees of freedom, enabling optical addressing of the K and K' valleys with the two circular polarizations [25–27]. An interesting consequence of these properties is the valley Hall effect [28,29], where shining a circularly polarized laser at a TMD monolayer at its band gap creates a population imbalance between the electron spin-states resulting in an effective magnetic field owing to the valley-dependent Berry curvature [30]. This effective magnetic field was shown to result in in-plane nonreciprocal plasmon transport [31,32]. Moreover, optically pumped TMD monolayers sandwiched in cavities were shown to achieve lasing [33–35], albeit from both valleys. In principle, it is possible to achieve circularly polarized lasing by pumping with the same circular polarization [26,27] or by injecting a spin-polarized current [36].

Circular polarization-dependent gain in TMD monolayers provides us a direct means to construct the dielectric tensor of Eq. (2). Consider the structure in Fig. 3 consisting of molybdenum disulfide (MoS_2) monolayers encapsulated by a layer of hexagonal boron nitride (hBN). hBN is a commonly used encapsulation layer in van der Waals heterostructures [37–39] and serves to maintain the broken inversion symmetry in MoS_2 required to utilize its valley-dependent properties. At room temperature and a frequency of 1.95 eV (636 nm) that is slightly above its band gap of
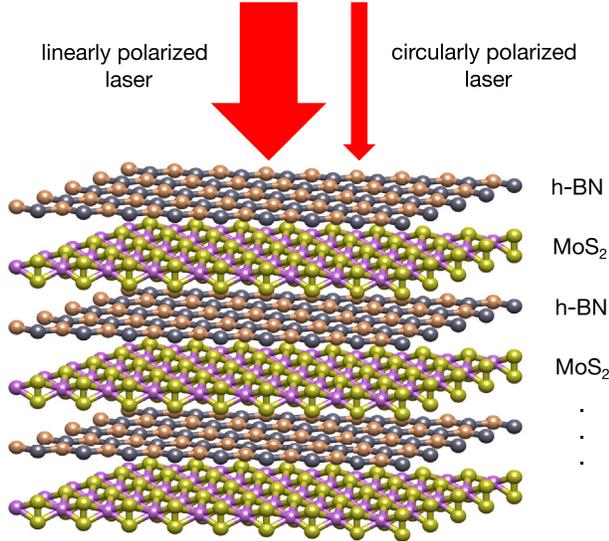
FIG. 3. A layered van der Waals heterostructure to realize the dielectric tensor of Eq. (2) for the case of $\epsilon_{xy} = -\epsilon_{yx}$. The linearly polarized laser shining on the heterostructure provides uniform gain for both valleys of MoS$_2$ while the circularly polarized laser provides a small, additional gain for only one valley.

1.9 eV (653 nm), an MoS$_2$ monolayer is described by an in-plane dielectric constant of $\epsilon_{xx} = \epsilon_{yy} = 24.269 - 11.113i$ and a layer thickness of 6.15 Å [40]. For hBN, we use a dielectric constant $\epsilon_{xx} = \epsilon_{yy} = 4.855$ with a layer thickness of 3.17 Å [41]. In principle, one of the two valleys of MoS$_2$ can be completely inverted by pumping using a circularly polarized laser, resulting in strong optical gain. However, since such strong gain in TMD monolayers is yet to be demonstrated [42], we assume that the MoS$_2$ monolayer is first uniformly pumped using a $|x\rangle$-polarized laser at 1.95 eV (636 nm) to $\epsilon_{xx} = \epsilon_{yy} = 24.269 - 1i$. Subsequently, a right-circularly polarized laser at the same frequency induces a gain of $+1i$ for one of the two valleys. In the circular-polarization basis, the in-plane dielectric tensor of the pumped MoS$_2$ monolayer is

$$\epsilon_\perp^{cc} = \begin{pmatrix} 24.269 + 1i & 0 \\ 0 & 24.269 - 1i \end{pmatrix}. \qquad (7)$$

By a unitary transform, this dielectric tensor can be converted to the x-y basis:

$$\epsilon_\perp = \begin{pmatrix} 24.269 & -1 \\ 1 & 24.269 \end{pmatrix}. \qquad (8)$$

To derive the dielectric tensor of the heterostructure of Fig. 3, we employ effective medium theory [43]. The effective medium approximation is valid in the deep-subwavelength limit, applicable here since the unit cell consisting of one MoS$_2$ monolayer and one hBN monolayer is significantly thinner than the operating wavelength

of 636 nm. In this approximation, the effective dielectric tensor of the van der Waals heterostructure of Fig. 3 is

$$\epsilon_\perp = \begin{pmatrix} \epsilon_r & \epsilon_{xy} \\ \epsilon_{yx} & \epsilon_r \end{pmatrix}, \qquad \epsilon_r = 17.6657,$$

$$\epsilon_{xy} = -\epsilon_{yx} = -0.6598, \qquad (9)$$

which is in the form expected by Eq. (2). A comparison of these values with parameter retrieval [44] from an exact transfer matrix calculation with 1000 unit cells resulted in a difference of less than 0.1%, confirming the predictions of effective medium theory in this deep subwavelength limit. Further, while the dielectric constants of 2D materials change by a few percent from monolayer to bulk [40], the valley-dependent gain or loss exploited in this Letter depend only on the broken inversion symmetry of the metamaterial. Therefore, the time-reversal symmetric form of the dielectric tensor of Eq. (9) remains valid up to a few percent change in its matrix elements. While the preceding analysis was performed at a single frequency slightly above the MoS$_2$ band gap, at carrier densities of about 5×10^{13}/cm^2, the gain bandwidth of monolayer MoS$_2$ is about 150 meV while that of WS$_2$ is about 200 meV [45]. Moreover, the bandwidth of the gain can be tuned by varying the pump laser intensity and the resultant carrier density. In addition, by engineering the sub- and superstrate dielectric environments, the band gaps of such monolayer TMDs can be tuned by hundreds of meVs [46,47]. Therefore, with the appropriate choice of the TMD, its carrier density, and the dielectric environment, the operating frequency and bandwidth of the resultant meta-material can be tuned significantly.

Thus far, we have constructed a metamaterial that realizes Eq. (2) with $\epsilon_{xy} = -\epsilon_{yx}$. To implement the general form of Eq. (2), we insert an anisotropic 2D material layer into the heterostructure. Several choices for such in-plane anisotropy exist [48–52]. Since the anisotropic layer should be nearly lossless at the operating wavelength of 1.95 eV (636 nm), SiP [50] or GeP [51], which have direct band gaps around 2.5 eV (496 nm), are good candidates. In general, lossless materials possessing an in-plane anisotropy are represented by

$$\epsilon_\perp = \begin{pmatrix} \epsilon_r' & \delta \\ \delta & \epsilon_r' \end{pmatrix}, \qquad \epsilon_r', \delta \in \mathbb{R}, \qquad (10)$$

where δ is the degree of anisotropy. Consider an effective medium constructed using the $\mathcal{T}$-symmetric metamaterial of Eq. (9) and the anisotropic layers of Eq. (10). In the resulting effective-medium tensor, the elements ϵ_{xy} of Eq. (9) and δ of Eq. (10) add in one of the off-diagonal components but subtract in the other, achieving two real but unequal off-diagonal components. Furthermore, by appropriately by varying the gain in the MoS$_2$ monolayer or the number of anisotropic monolayers, it is possible to have both off-diagonal components of the same sign for $\tau > 0$.

Therefore, the general form of Eq. (2) can be achieved by a van der Waals heterostructure consisting of TMD monolayers pumped with circularly polarized light, in-plane anisotropic media such as SiP or GeP, and/or encapsulation layers such as hBN.

Discussion.—In this Letter, we explore a new class of non-Hermitian, nonreciprocal metamaterials that preserve time-reversal symmetry. From their polarization dynamics, we highlight their unique properties such as polarization- and direction-dependent gain and loss that enables two-way signal amplification while simultaneously attenuating back-reflections in both directions. We further propose a design for such metamaterials in the form of van der Waals heterostructures comprising 2D materials such as transition metal dichalcogenides (TMDs) and anistropic monolayers. More generally, nonreciprocal designs based on 2D materials, such as the ones proposed in this Letter, allow for large-area nonreciprocity, providing a potential advantage over nonreciprocity arising from time-modulated systems [53–55] that are constrained in their cross-sectional area. Furthermore, the strength of the nonreciprocity depends only on the ability to pump TMD monolayers using circularly polarized lasers, unlike magneto-optical systems where substantial external magnetic fields may be required to observe significant nonreciprocity.

[1] D. R. Smith, J. B. Pendry, and M. C. Wiltshire, Science **305,** 788 (2004).

[2] A. Alù and N. Engheta, Phys. Rev. E **72,** 016623 (2005).

[3] N. Engheta and R. W. Ziolkowski, *Metamaterials: Physics and Engineering Explorations* (John Wiley & Sons, New York, 2006).

[4] V. M. Shalaev, Nat. Photonics **1,** 41 (2007).

[5] H. N. Krishnamoorthy, Z. Jacob, E. Narimanov, I. Kretzschmar, and V. M. Menon, Science **336,** 205 (2012).

[6] A. M. Mahmoud, A. R. Davoyan, and N. Engheta, Nat. Commun. **6,** 8359 (2015).

[7] A. Poddubny, I. Iorsh, P. Belov, and Y. Kivshar, Nat. Photonics **7,** 948 (2013).

[8] T. Xu, A. Agrawal, M. Abashin, K. J. Chau, and H. J. Lezec, Nature (London) **497,** 470 (2013).

[9] F. Monticone and A. Alu, J. Mater. Chem. C **2,** 9059 (2014).

[10] See the Supplemental Material at http://link.aps.org/supplemental/10.1103/PhysRevLett.124.257403 for detailed derivations relating to the permittivity tensor considered here and the polarization-dependent two-way directional amplifier, which includes Ref. [11].

[11] H. A. Haus, *Waves and Fields in Optoelectronics* (Prentice-Hall, Englewood Cliffs, 1984).

[12] A. Cerjan and S. Fan, Phys. Rev. Lett. **118,** 253902 (2017).

[13] R. El-Ganainy, K. G. Makris, M. Khajavikhan, Z. H. Musslimani, S. Rotter, and D. N. Christodoulides, Nat. Phys. **14,** 11 (2018).

[14] B. Abdo, K. Sliwa, L. Frunzio, and M. Devoret, Phys. Rev. X **3,** 031001 (2013).

[15] F. Ruesink, M.-A. Miri, A. Alu, and E. Verhagen, Nat. Commun. **7,** 13662 (2016).

[16] A. Kamal and A. Metelmann, Phys. Rev. Applied **7,** 034031 (2017).

[17] T. T. Koutserimpas and R. Fleury, Phys. Rev. Lett. **120,** 087401 (2018).

[18] D. Malz, L. D. Tóth, N. R. Bernier, A. K. Feofanov, T. J. Kippenberg, and A. Nunnenkamp, Phys. Rev. Lett. **120,** 023601 (2018).

[19] L. Mercier de Lépinay, E. Damskägg, C. F. Ockeloen-Korppi, and M. A. Sillanpää, Phys. Rev. Applied **11,** 034027 (2019).

[20] A. Y. Song, Y. Shi, Q. Lin, and S. Fan, Phys. Rev. A **99,** 013824 (2019).

[21] N. Hatano and D. R. Nelson, Phys. Rev. Lett. **77,** 570 (1996).

[22] S. Longhi, D. Gatti, and G. Della Valle, Sci. Rep. **5,** 13376 (2015).

[23] S. Longhi, D. Gatti, and G. Della Valle, Phys. Rev. B **92,** 094204 (2015).

[24] K. F. Mak, C. Lee, J. Hone, J. Shan, and T. F. Heinz, Phys. Rev. Lett. **105,** 136805 (2010).

[25] H. Zeng, J. Dai, W. Yao, D. Xiao, and X. Cui, Nat. Nanotechnol. **7,** 490 (2012).

[26] K. F. Mak and J. Shan, Nat. Photonics **10,** 216 (2016).

[27] K. F. Mak, D. Xiao, and J. Shan, Nat. Photonics **12,** 451 (2018).

[28] K. F. Mak, K. L. McGill, J. Park, and P. L. McEuen, Science **344,** 1489 (2014).

[29] J. R. Schaibley, H. Yu, G. Clark, P. Rivera, J. S. Ross, K. L. Seyler, W. Yao, and X. Xu, Nat. Rev. Mater. **1,** 16055 (2016).

[30] D. Xiao, M.-C. Chang, and Q. Niu, Rev. Mod. Phys. **82,** 1959 (2010).

[31] J. C. Song and M. S. Rudner, Proc. Natl. Acad. Sci. U.S.A. **113,** 4658 (2016).

[32] A. Kumar, A. Nemilentsau, K. H. Fung, G. Hanson, N. X. Fang, and T. Low, Phys. Rev. B **93,** 041413(R) (2016).

[33] Y. Ye, Z. J. Wong, X. Lu, X. Ni, H. Zhu, X. Chen, Y. Wang, and X. Zhang, Nat. Photonics **9,** 733 (2015).

[34] O. Salehzadeh, M. Djavid, N. H. Tran, I. Shih, and Z. Mi, Nano Lett. **15,** 5302 (2015).

[35] Y. Li, J. Zhang, D. Huang, H. Sun, F. Fan, J. Feng, Z. Wang, and C.-Z. Ning, Nat. Nanotechnol. **12,** 987 (2017).

[36] J. Rudolph, D. Hägele, H. Gibbs, G. Khitrova, and M. Oestreich, Appl. Phys. Lett. **82,** 4516 (2003).

[37] A. K. Geim and I. V. Grigorieva, Nature (London) **499**, 419 (2013).

[38] S. Dai, Q. Ma, M. Liu, T. Andersen, Z. Fei, M. Goldflam, M. Wagner, K. Watanabe, T. Taniguchi, M. Thiemens *et al.*, Nat. Nanotechnol. **10**, 682 (2015).

[39] K. Novoselov, A. Mishchenko, A. Carvalho, and A. C. Neto, Science **353**, aac9439 (2016).

[40] Y. Li, A. Chernikov, X. Zhang, A. Rigosi, H. M. Hill, A. M. van der Zande, D. A. Chenet, E.-M. Shih, J. Hone, and T. F. Heinz, Phys. Rev. B **90**, 205422 (2014).

[41] A. Laturia, M. L. Van de Put, and W. G. Vandenberghe, npj 2D Mater. Appl. **2**, 6 (2018).

[42] A. Chernikov, C. Ruppert, H. M. Hill, A. F. Rigosi, and T. F. Heinz, Nat. Photonics **9**, 466 (2015).

[43] V. Agranovich and V. Kravtsov, Solid State Commun. **55**, 85 (1985).

[44] D. R. Smith, D. C. Vier, T. Koschny, and C. M. Soukoulis, Phys. Rev. E **71**, 036617 (2005).

[45] F. Lohof, A. Steinhoff, M. Florian, M. Lorke, D. Erben, F. Jahnke, and C. Gies, Nano Lett. **19**, 210 (2018).

[46] M. M. Ugeda, A. J. Bradley, S.-F. Shi, H. Felipe, Y. Zhang, D. Y. Qiu, W. Ruan, S.-K. Mo, Z. Hussain, Z.-X. Shen *et al.*, Nat. Mater. **13**, 1091 (2014).

[47] A. Raja, A. Chaves, J. Yu, G. Arefe, H. M. Hill, A. F. Rigosi, T. C. Berkelbach, P. Nagler, C. Schüller, T. Korn *et al.*, Nat. Commun. **8**, 15251 (2017).

[48] V. Tran, R. Soklaski, Y. Liang, and L. Yang, Phys. Rev. B **89**, 235319 (2014).

[49] F. Xia, H. Wang, and Y. Jia, Nat. Commun. **5**, 4458 (2014).

[50] S. Zhang, S. Guo, Y. Huang, Z. Zhu, B. Cai, M. Xie, W. Zhou, and H. Zeng, 2D Mater. **4**, 015030 (2016).

[51] L. Li, W. Wang, P. Gong, X. Zhu, B. Deng, X. Shi, G. Gao, H. Li, and T. Zhai, Adv. Mater. **30**, 1706771 (2018).

[52] L. Li, P. Gong, D. Sheng, S. Wang, W. Wang, X. Zhu, X. Shi, F. Wang, W. Han, S. Yang *et al.*, Adv. Mater. **30**, 1804541 (2018).

[53] Z. Yu and S. Fan, Nat. Photonics **3**, 91 (2009).

[54] K. Fang, Z. Yu, and S. Fan, Phys. Rev. Lett. **108**, 153901 (2012).

[55] D. L. Sounas and A. Alù, Nat. Photonics **11**, 774 (2017).